

## Supporting Information

### Evidence for the formation of a mononuclear ferric-hydroperoxo complex via the reaction of dioxygen with an (N<sub>4</sub>S(thiolate))iron(II) complex

Yunbo Jiang,<sup>a</sup> Joshua Telser<sup>b</sup> and David P. Goldberg\*<sup>a</sup>

<sup>a</sup>Department of Chemistry, Johns Hopkins University, Baltimore, Maryland, 21218, USA

<sup>b</sup> Chemistry Program, Roosevelt University, Chicago, IL 60605 USA

#### Contact Information

Professor David P. Goldberg

Department of Chemistry

Johns Hopkins University, Baltimore, Maryland, 21218, USA

Tel: 410-516-6658

Fax: 410-516-8420

E-mail: dpg@jhu.edu

**General Procedures.** All reactions were carried out under an atmosphere of N<sub>2</sub> or Ar using a drybox or standard Schlenk techniques. 1,4,8,12-tetraazocyclopentadecane ([15]aneN<sub>4</sub>) (98%) was purchased from Strem Chemicals. Thiophenol (97%) and 4-chlorothiophenol (98%) were purchased from Acros. Iron(II) tetrafluoroborate hexahydrate (97%) and sodium hydride (60%, dispersion in mineral oil) were purchased from Aldrich. All other reagents were purchased from commercial vendors and used without further purification unless noted otherwise. Diethyl ether and dichloromethane were purified via a Pure-Solv Solvent Purification System from Innovative Technology, Inc. Propionitrile and methanol were distilled over CaH<sub>2</sub> [1]. All solvents were degassed by repeated cycles of freeze-pump-thaw and then stored in a drybox. Dioxygen gas (2.6 Grade) was purchased from BOC Gases, and <sup>18</sup>O<sub>2</sub> (98%) was purchased from Icon Isotopes, Inc. The complexes [Fe<sup>II</sup>([15]aneN<sub>4</sub>)(SC<sub>6</sub>H<sub>4</sub>-*p*-Cl)]BF<sub>4</sub> (**1**) and [Fe<sup>II</sup>(Me<sub>4</sub>[15]aneN<sub>4</sub>)(SC<sub>6</sub>H<sub>5</sub>)]BPh<sub>4</sub> (**3**) were prepared as described elsewhere [2,3].

**Physical Methods.** UV-visible spectra were recorded on a Cary 50 Bio spectrophotometer equipped with a fiber-optic coupler (Varian) and an all-quartz immersion probe (Hellma 661.202-UV, 2 mm path length), using custom-made Schlenk tubes designed to house the immersion probe. Electron paramagnetic resonance (EPR) spectra were obtained on a Bruker EMX EPR spectrometer controlled with a Bruker ER 041 X G microwave bridge at 10 K. The EPR spectrometer was equipped with a continuous-flow liquid He cryostat and an ITC503 temperature controller made by Oxford Instruments, Inc. Electrospray ionization mass spectra (ESI MS) were collected on a Thermo Finnigan LCQ Deca ion trap mass spectrometer by infusing samples directly into the source at 20 μL/min using a syringe pump. The spray voltage was set at 5 kV and the capillary temperature was held at 150 °C. Infra-red spectroscopy was measured with a Nicolet NEXUS 670 FT-IR instrument with NaCl plates.

**Formation of the Fe<sup>III</sup>-OOH complex (2). UV-vis spectroscopy.** [Fe<sup>II</sup>([15]aneN<sub>4</sub>)(SPh-*p*-Cl)]BF<sub>4</sub> (**1**) (10 mg, 0.02 mmol) was loaded into a custom-made Schlenk tube and dissolved in CH<sub>3</sub>CH<sub>2</sub>CN (10 mL). An all-quartz immersion probe for low-temperature UV-vis spectroscopy was inserted into the tube, and the solution was cooled to -78 °C. After

cooling to the desired temperature, O<sub>2</sub>(g) was bubbled continuously through the solution for 3 min, resulting in an immediate color change from colorless to deep red. The reaction was monitored by UV-vis spectroscopy and formation of **2** was observed by the appearance of a band at 460 nm ( $\epsilon \sim 2100 \text{ M}^{-1} \text{ cm}^{-1}$ , based on total Fe). The peak at 460 nm was monitored over time and slowly decayed over 1.5 h.

**EPR spectroscopy.** A thick-walled (2.4-mm inner diameter, 4-mm outer diameter) suprasil EPR tube (Wilmad, 727-SQ-250M) containing a solution of [Fe<sup>II</sup>([15]aneN<sub>4</sub>)(SPh-*p*-Cl)]BF<sub>4</sub> (**1**) (2.3 mM) in CH<sub>3</sub>CH<sub>2</sub>CN (300  $\mu$ L) was cooled to -78 °C, and O<sub>2</sub>(g) was bubbled through this solution for 2 min. An immediate color change from colorless to deep red was observed. Bubbling of O<sub>2</sub>(g) for longer time periods (7 – 50 min) resulted in a progressive loss of the intensity of the red chromophore as observed by eye (Figure S1). Samples for EPR were sparged with N<sub>2</sub>(g) to remove any excess O<sub>2</sub>(g) prior to slow annealing and storage at 77 K before taking EPR measurements. *Caution: frozen tubes of propionitrile easily explode upon warming, and thawing of these tubes should be done with care.* Quantitation of the LS Fe<sup>III</sup> EPR signal for **2** was carried out by double integration under nonsaturating conditions (microwave power, 0.2 mW), followed by comparison with a calibration curve constructed from a series of Cu<sup>II</sup>(EDTA) standard solutions (0.2, 1.0 and 5.1 mM) [4]. The yield of **2** was found to be 40  $\pm$  5% by this method (3 independent samples).

**ESI mass spectroscopy.** [Fe<sup>II</sup>([15]aneN<sub>4</sub>)(SPh-*p*-Cl)]BF<sub>4</sub> (**1**) (5 mg, 0.01 mmol) was loaded in a Schlenk flask and dissolved in CH<sub>3</sub>CH<sub>2</sub>CN (10 mL) to give a final concentration of 1 mM of the Fe<sup>II</sup> complex. After cooling to -78 °C, O<sub>2</sub>(g) was bubbled through the solution for  $\sim$ 3 min, resulting in the rapid formation of the deep red color of **2**. Samples of the reaction mixture were rapidly injected by using a pre-cooled syringe and infused into the source at 20  $\mu$ L/min via syringe pump. Care must be taken to generate fresh solutions of **2** immediately prior to injection. Pre-cooling of the syringe can be carried out by immersion in dry ice or liquid nitrogen, but significant decomposition of **2** in the syringe is unavoidable, as noted by the conversion of the red color to a brownish decomposition product. Injection into the instrument must be done as fast

as possible. The full range ESIMS for **2** is shown in Figure S5 together with the spectrum for the starting material **1** for comparison. A dominant peak at  $m/z$  268 is observed for both species. The molecular ion at  $m/z$  443.9 is relatively low in abundance compared to  $m/z$  268, but this is not surprising given the inherent thermal instability of **2**.

**Summary of theoretical treatment for determining the ligand-field parameters from  $g$  values of LS Fe<sup>III</sup>-OO(H or R) complexes.** We have chosen to use the method of McGarvey[5,6] for the analysis of the EPR parameters for complex **2**. For comparison, we have also recalculated the parameters for the series of Fe<sup>III</sup>-OO(H or R) complexes previously analyzed in Girerd et al.[7] in which the method of Griffith and Taylor was used. We believe, however, that the McGarvey model provides the most accurate theoretical treatment.

In this model, the ground state doublet wave functions for the LS Fe<sup>III</sup> complexes ( $\Psi_{\pm}$  in the  $(d_{xz}, d_{yz}, d_{xy})^5$  basis set) are defined as follows:

$$\Psi_+ = A |d_{xy}^+\rangle + B |d_{yz}^-\rangle + C |d_{xz}^-\rangle, \Psi_- = -A |d_{xy}^-\rangle + B |d_{yz}^+\rangle - C |d_{xz}^+\rangle \quad (1)$$

where:

$$|d_{xy}^{\pm}\rangle = [d_{xz}^+ d_{xz}^- d_{yz}^+ d_{yz}^- d_{xy}^{\pm}], |d_{xz}^{\pm}\rangle = i [d_{yz}^+ d_{yz}^- d_{xy}^+ d_{xy}^- d_{xz}^{\pm}], |d_{yz}^{\pm}\rangle = [d_{xz}^+ d_{xz}^- d_{xy}^+ d_{xy}^- d_{yz}^{\pm}] \quad (2)$$

The wavefunction coefficients give the following equations for the  $g$  values:

$$g_x = 2[B^2 - A^2 - C^2 - 2kAC]; g_y = 2[C^2 - B^2 - A^2 - 2kAB]; g_z = 2[A^2 - C^2 - B^2 - 2kBC] \quad (3)$$

It can be seen from Eqns 3 that a given  $g$  value in a LS  $d^5$  system can be either positive or negative. If the sign of  $g$  is not determined experimentally (which is normally the case), then the McGarvey model yields two solutions for the  $g$  values. One of these solutions, however, can usually be eliminated based on physical knowledge of the system under study. The wavefunction coefficients also provide the normalized values of  $\Delta$  (the tetragonal distortion; trigonal distortion is not considered in our study) and  $V$  (the rhombic distortion):

$$\Delta/\zeta = [A(1 - A^2) + (B + C)(1 - (B + C)^2)]/(4ABC); V/\zeta = [(A + B + C)(C - B)]/(2BC) \quad (4)$$

These parameters are defined so that  $|d_{xy}^{\pm}\rangle$  is at energy  $\Delta$  and  $|d_{xz}^{\pm}\rangle$  and  $|d_{yz}^{\pm}\rangle$  are at energies  $(2\Delta -$

$V/2$ ) and  $(2\Delta + V/2)$ , respectively (disregarding spin-orbit coupling). There is the constraint that  $|\Delta| \geq (2/3)|V|$ , otherwise the coordinate system must be redefined. These ligand-field distortion parameters are normalized by the one-electron spin-orbit coupling constant,  $\zeta$ , which equals  $427 \text{ cm}^{-1}$  for free-ion  $\text{Fe}^{3+}$  [8]. The energy level diagrams illustrating  $\Delta$  and  $V$  in both the “hole” and five electron formalisms are given in Figure S3.

**Fitting procedure and results.** The experimental  $g$  values (as magnitudes) were inputted into a locally written program (DLSD5, available from J. Telser) that applies Eqns 3 in an iterative process to yield best fit agreement between experimental and calculated  $g$  values. The output comprises the sign and assignment with respect to  $x, y, z$  of the calculated  $g$  values, and the values of the wavefunction coefficients and ligand-field splittings (from Eqns 4). Two solutions for illustration are obtained, and are presented in Table S1 for **2** and for two LS Fe(III) complexes taken from Table 3 of McGarvey [6]. The first solution (first row for each complex) is not physically reasonable for these complexes because it requires very small tetragonal distortion ( $|\Delta| < \sim 100 \text{ cm}^{-1}$ ) in these highly structurally distorted complexes. The second solution is the physically meaningful one (marked by an asterisk), in which the product  $g_x g_y g_z$  is positive.

The EPR parameters for **2** along with a series of  $\text{Fe}^{\text{III}}$ -OO(H or R) complexes previously analyzed in the review by Girerd *et al.*[7] are listed in Table S2 for comparison. Also included are results for the thiolate-ligated complexes  $[\text{Fe}(\text{S}^{\text{Me}_2}\text{N}_4(\text{tren}))(\text{OOH})]^+$ [9] and  $[\text{Fe}([15]\text{aneN}_4)(\text{SC}_6\text{H}_5)(\text{OO}t\text{-Bu})]^+$  [2]. It should be noted that there are two typographical errors in Table 2 of Girerd *et al.* that we have corrected here. The  $g_{\text{max}}$  and  $g_{\text{mid}}$  values for  $[\text{Fe}(\text{phen})_2(\text{MeOH})(\text{OO}t\text{-Bu})]^{2+}$  appear to have been interchanged. The  $g_{\text{min}}$  value for  $[(\text{TPEN})\text{Fe}(\text{OOH})]^{2+}$  is given as 1.967 in the original work [10], but is listed as 1.997 in Girerd *et al.*, which gives very unreasonable fit values. The ligand-field parameters obtained in Table S2 are quite reasonable. The fit values of  $k$  are slightly less than unity (generally  $0.8 < k < 1.0$ ), which is as expected for the orbital reduction effect due to covalency. The values for  $\Delta$  are on the order of  $4000 \text{ cm}^{-1}$  and are generally somewhat smaller (by  $\sim 15 - 20 \%$ ) than those derived by Girerd *et al.*, which makes them more in line with LS Fe(III) porphyrins [6].

Two comments regarding complex **2** can be made in the context of the tabulated results. The first is that although  $g_{\max}$  and  $g_{\text{mid}}$  are larger in magnitude than those for the other (hydro)peroxo complexes listed,  $g_{\min}$  is generally smaller so that the electronic structure as given by the normalized ligand-field parameters is almost exactly the same as, e.g., (BLM)Fe(OOH) and [(trispicMeen)Fe(OOH)]<sup>2+</sup>. However for **2**,  $k > 1$  (1.139), which leads to the larger  $|g|$  spread. We speculate that this might be due to the axial thiolate ligand in that spin-orbit coupling effects involving the relatively heavier S atom would lead to a larger orbital contribution than for complexes with only light atom (N, O) ligation. For our previously reported thiolate-ligated complex [Fe([15]aneN<sub>4</sub>)(SC<sub>6</sub>H<sub>5</sub>)(OO*t*-Bu)]<sup>+</sup> [2], the present analysis shows that its value for tetragonal splitting is in line with other such complexes ( $\Delta/\zeta \approx 10$ ), but its value for  $k$  is also relatively large (1.149). More sophisticated computational studies are needed to probe this effect.

## References

- [1] *Purification of Laboratory Chemicals*; W. L. F. Armarego, D. D. Perrin, Butterworth-Heinemann, Oxford, 1996.
- [2] F. Namuswe, G. D. Kasper, A. A. N. Sarjeant, T. Hayashi, C. M. Krest, M. T. Green, P. Moënne-Loccoz and D. P. Goldberg, *J. Am. Chem. Soc.*, 2008, **130**, 14189-14200.
- [3] F. Namuswe, T. Hayashi, G. D. Kasper, A. A. N. Sarjeant, P. Moënne-Loccoz, and D. P. Goldberg, submitted for publication.
- [4] F. Bou-Abdallah, N. D. Chasteen. *J. Biol. Inorg. Chem.*, 2008, **13**, 15-24.
- [5] B. R. McGarvey, *Quim. Nova*, 1998, **21**, 206-213.
- [6] B. R. McGarvey, *Coord. Chem. Rev.*, 1998, **170**, 75-92.
- [7] J. J. Girerd, F. Banse and A. J. Simaan, *Struct. Bonding*, 2000, **97**, 145-177.
- [8] J. Bendix, M. Brorson, C. E. Schaffer, *Inorg. Chem.*, 1993, **32**, 2838-2849.
- [9] J. Shearer, R. C. Scarrow and J. A. Kovacs, *J. Am. Chem. Soc.*, 2002, **124**, 11709-11717.
- [10] A. J. Simaan, S. Döpner, F. Banse, S. Bourcier, G. Bouchoux, A. Boussac, P. Hildebrandt and J. J. Girerd, *Eur. J. Inorg. Chem.*, 2000, 1627-1633.

**Table S1.** EPR-derived parameters for **2** and two LS Fe(III) complexes showing both solutions obtained using the McGarvey model [5.6].

Complex	$g_{\min}$ ( $g_z$ )	$g_{\text{mid}}$ ( $g_y$ )	$g_{\max}$ ( $g_x$ )	$A$ ( $d_{xy}$ )	$B$ ( $d_{yz}$ )	$C$ ( $d_{xz}$ )	$k$	$\Delta/\zeta$	$V/\zeta$
<b>(2)</b>	-1.940	-2.239	-2.347	0.6094	0.5531	0.5680	1.134	0.124	0.041
	* +1.940	-2.239	-2.347	0.9951	0.0583	0.0795	1.139	7.852	2.596
<i>cis</i> -[Fe(bpy) <sub>2</sub> (CN) <sub>2</sub> ] <sup>+</sup>	-1.54	-2.47	-2.74	0.6700	0.5065	0.5428	1.214	0.357	0.113
	* +1.54	-2.47	-2.74	0.9607	0.1701	0.2196	1.014	2.820	0.895
<i>cis</i> -[Fe(phen) <sub>2</sub> (CN) <sub>2</sub> ] <sup>+</sup>	-1.42	-2.63	-2.63	0.6828	0.5166	0.5166	1.203	0.404	0.000
	* +1.42	-2.63	-2.63	0.9502	0.2204	0.2204	0.9840	2.423	0.000

\* The favored solution based on ligand-field parameters.

**Table S2.** EPR-derived parameters for LS Fe<sup>III</sup>-OO(H or R) complexes taken from Girerd et al.[7] and related thiolate-ligated complexes [2, 9].

Hydroperoxo Complex	$g_{\min}$ ( $g_z$ )	$g_{\text{mid}}$ ( $g_y$ )	$g_{\max}$ ( $g_x$ )	$A$ ( $d_{xy}$ )	$B$ ( $d_{yz}$ )	$C$ ( $d_{xz}$ )	$k$	$\Delta/\zeta$	$V/\zeta$
<b>(2)</b>	+1.940	-2.239	-2.347	0.9951	0.0583	0.0795	1.139	7.852	2.596
(BLM)Fe(OOH)	+1.94	-2.17	-2.26	0.9946	0.0608	0.0842	0.8198	7.493	2.605
[(trispicMeen)Fe(OOH)] <sup>2+</sup>	+1.95	-2.12	-2.19	0.9952	0.0570	0.0796	0.6404	7.947	2.818
[(trispicen)Fe(OOH)] <sup>2+</sup>	+1.96	-2.14	-2.19	0.9963	0.0529	0.0673	0.7500	8.863	2.259
[(TPEN)Fe(OOH)] <sup>2+</sup>	+1.967	-2.15	-2.22	0.9971	0.0443	0.0612	0.9329	10.165	3.430
[(bztpen)Fe(OOH)] <sup>2+</sup>	+1.96	-2.16	-2.20	0.9964	0.0541	0.0648	0.8198	8.897	1.700
[(TPA)Fe(OOH)] <sup>2+</sup>	+1.96	-2.15	-2.19	0.9964	0.0543	0.0656	0.7723	8.833	1.762
[(N4py)Fe(OOH)] <sup>2+</sup>	+1.98	-2.12	-2.17	0.9983	0.0350	0.0474	0.9240	12.886	4.056
[(Py5)Fe(OOH)] <sup>2+</sup>	+1.98	-2.13	-2.15	0.9983	0.0390	0.0442	0.8846	12.506	1.623
[Fe(bpy) <sub>2</sub> (py)(OOH)] <sup>2+</sup>	+1.97	-2.11	-2.14	0.9972	0.0481	0.0582	0.6435	9.922	1.976
[Fe(phen) <sub>2</sub> (py)(OOH)] <sup>2+</sup>	+1.97	-2.12	-2.13	0.9972	0.0516	0.0549	0.6418	9.816	0.652
[(PMA)Fe(OOH)] <sup>+</sup>	+1.94	-2.17	-2.22	0.9945	0.0668	0.0809	0.7387	7.231	1.497

Alkylperoxo Complex	$g_{\min}$ ( $g_z$ )	$g_{\text{mid}}$ ( $g_y$ )	$g_{\max}$ ( $g_x$ )	$A$ ( $d_{xy}$ )	$B$ ( $d_{yz}$ )	$C$ ( $d_{xz}$ )	$k$	$\Delta/\zeta$	$V/\zeta$
"[(Me,Me, <i>m</i> -xyl)Fe(OOH)]"	+1.93	-2.16	-2.23	0.9934	0.0700	0.0906	0.6934	6.726	1.875
[Fe(S <sup>Me2</sup> N <sub>4</sub> (tren))(OOH)] <sup>+</sup> *	+1.97	-2.14	-2.14	0.9972	0.0525	0.0525	0.7212	9.945	0.000
Fe(TPA)(H <sub>2</sub> O)(OO <i>t</i> -Bu)] <sup>2+</sup>	+1.98	-2.14	-2.19	0.9984	0.0348	0.0457	1.067	13.108	3.697
[Fe(6-MeTPA)(H <sub>2</sub> O)(OO <i>t</i> -Bu)] <sup>2+</sup>	+1.97	-2.12	-2.20	0.9973	0.0403	0.0606	0.8408	10.731	4.711
[Fe(TPA)(HOCH <sub>2</sub> Ph)(OO <i>t</i> -Bu)] <sup>2+</sup>	+1.97	-2.12	-2.19	0.9973	0.0417	0.0609	0.8110	10.563	4.162
[Fe(PMA)(OO <i>t</i> -Bu)] <sup>+</sup>	+1.93	-2.18	-2.28	0.9937	0.0655	0.0912	0.8196	6.970	2.480
[Fe(bpy) <sub>2</sub> (HOCH <sub>2</sub> Ph)(OO <i>t</i> -Bu)] <sup>2+</sup>	+1.98	-2.12	-2.18	0.9983	0.0337	0.0481	0.9614	13.096	4.806
[Fe(bpy) <sub>2</sub> (py)(OO <i>t</i> -Bu)] <sup>2+</sup>	+1.97	-2.12	-2.19	0.9973	0.0417	0.0609	0.8110	10.563	4.162
[Fe(phen) <sub>2</sub> (py)(OO <i>t</i> -Bu)] <sup>2+</sup>	+1.96	-2.12	-2.165	0.9962	0.0539	0.0686	0.6462	8.704	2.221
[Fe(phen) <sub>2</sub> (MeOH)(OO <i>t</i> -Bu)] <sup>2+</sup>	+1.97	-2.16	-2.19	0.9974	0.0470	0.0544	0.9170	10.352	1.589
[Fe(6-PhTPA)(OO <i>t</i> -Bu)] <sup>2+</sup>	+1.97	-2.12	-2.19	0.9973	0.0417	0.0609	0.8110	10.563	4.162
[Fe([15]aneN <sub>4</sub> )(SC <sub>6</sub> H <sub>5</sub> )(OO <i>t</i> -Bu)] <sup>+</sup>	+1.969	-2.209	-2.226	0.9975	0.0479	0.0513	1.149	10.518	0.762

\*This complex is likely not rigorously axial, but the small rhombic splitting was not extracted in the original work.

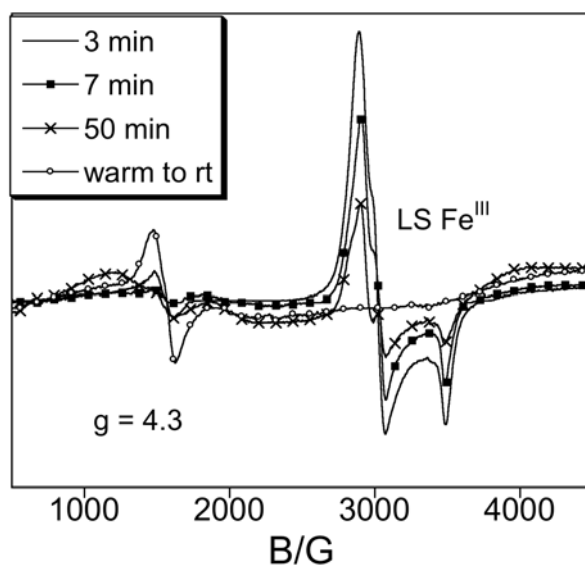


**Figure S1.** EPR spectra of **1** (2.2 mM) + O<sub>2</sub>(g) in CH<sub>3</sub>CH<sub>2</sub>CN with increasing amounts of time for bubbling of O<sub>2</sub>(g) at -78 °C, and the EPR spectrum after warming to room temperature. The increase over time in the lower-field feature due to HS Fe(III) and the concurrent decrease in the higher-field feature due to LS Fe(III) is apparent. Instrumental parameters: temperature, 10 K; frequency, 9.475 GHz; power 2 mW; modulation amplitude, 10 G.

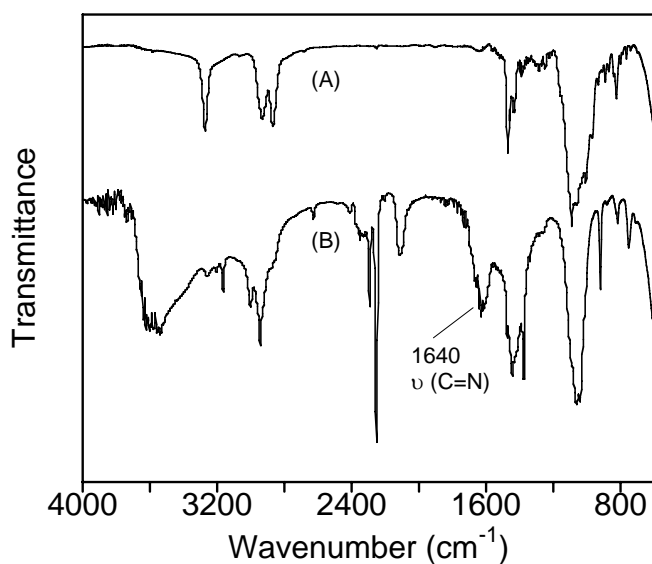


**Figure S2** FTIR spectra (thin film, NaCl plates) of **1** (A) and **1** + O<sub>2</sub>(g) in CH<sub>3</sub>CH<sub>2</sub>CN at -78 °C followed by warming to room temperature (B).

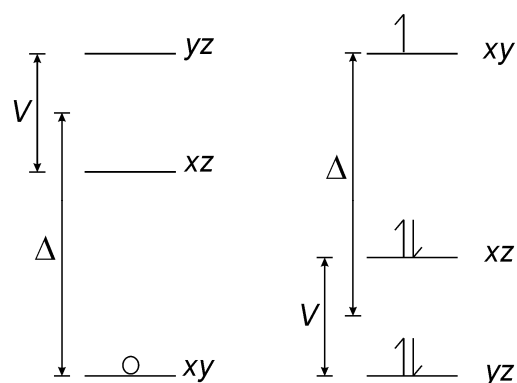


**Figure S3.** Energy levels for the  $t_2^5$  orbitals in a tetragonally distorted complex using the hole formalism (left) and the five electron formalism (right). The relative scaling of the levels roughly corresponds to the results found for **2**:  $\Delta/\zeta = 7.85$ ,  $V/\zeta = 2.60$ .

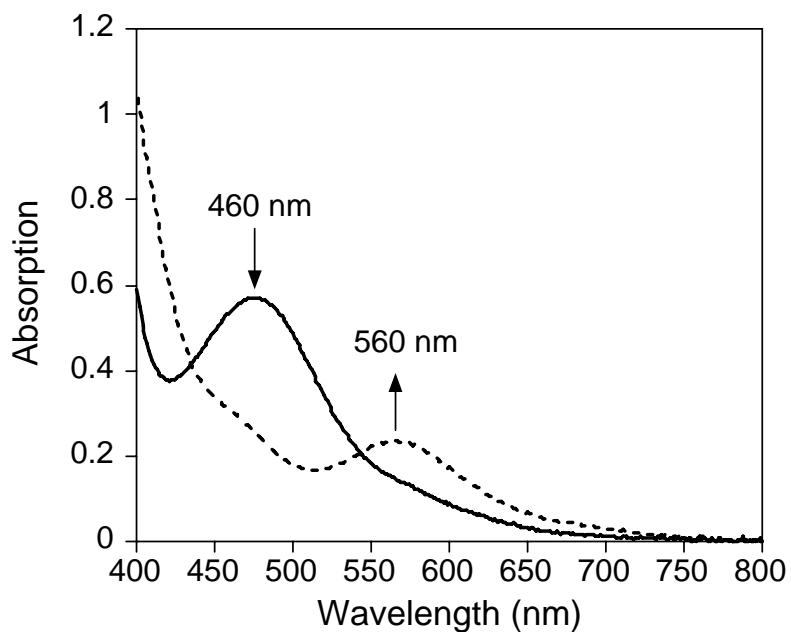
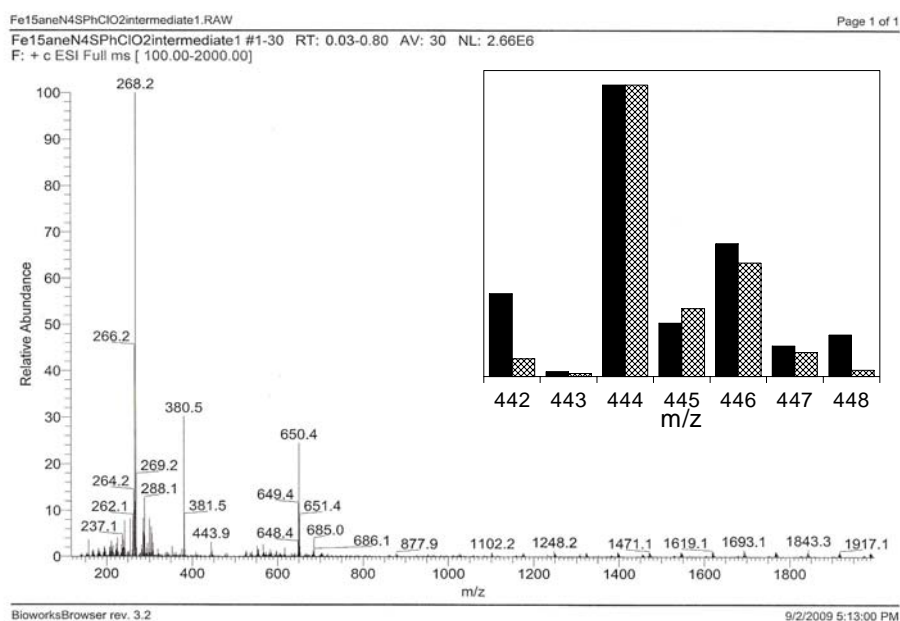


**Figure S4.** UV-Vis spectra of **2** in  $\text{CH}_3\text{CH}_2\text{CN}$  before (—) and after (---) the addition of 1 equiv of  $\text{PhCO}_2\text{H}$  at  $-78^\circ\text{C}$ . The 560 nm peak forms immediately after the addition, and then decays over several minutes to a brown solution with tailing absorption from 400 – 800 nm.

(a)



(b)

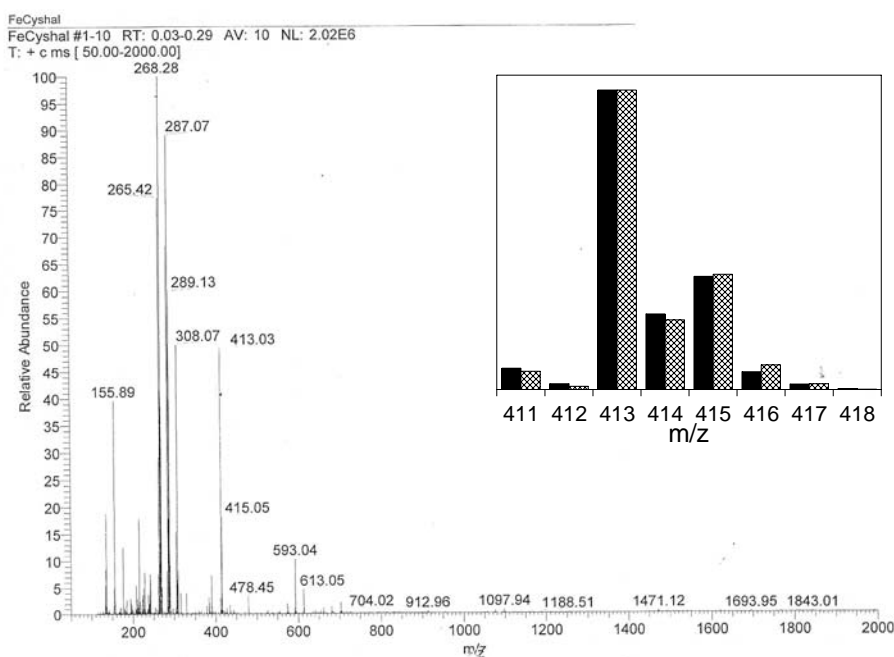


**Figure S5.** Full-range ESIMS of (a) **2** ( $m/z$  443.9) in  $\text{CH}_3\text{CH}_2\text{CN}$  and (b) **1** ( $m/z$  413.03) in  $\text{CH}_2\text{Cl}_2$ . Insets in (a) and (b) show observed (black) and theoretical (shadow) isotope distribution patterns. A dominant peak at  $m/z$  268 is observed for both species. The molecular ion at  $m/z$  443.9 is relatively low in abundance compared to  $m/z$  268, but this is not surprising given the inherent thermal instability of **2**.